ENPM 667 - Project # 1
University of Maryland, College Park

Enhanced Bioinspired Backstepping Control for a Mobile Robot with Unscented Kalman Filter

Team members:

Jayesh Jayashankar (117450101)
Aneesh Chodisetty (117359893)

Professor:

Dr. Waseem A. Malik

Table of Contents

Table of Equations

1. Introduction

The objectives as part of this project are to ensure that a mobile robot does not change its direction as it travels along a straight path by combining a bioinspired backstepping controller and a torque controller. A Kalman filter and an Unscented Kalman filter is used to ensure that the desired position is close to the estimated position. The stability is ensured by the Lyapunov stability analysis. The report covers details of the Mobile Robot's Kinematics and Dynamics, computation of the estimated state, Kalman Gain and Error covariance of the Kalman Filter and Unscented Kalman Filter, deriving the velocities and torque parameters of the backstepping and torque controller followed by an overview of the Lyapunov stability analysis. The block diagram of the tracking algorithm has been setup in Simulink with simulations being forward for a mobile robot travelling in a straight path.

2. Background

The inspiration for the project is drawn from [1] which uses the model of a non-holonomic mobile robot as in Figure 1.

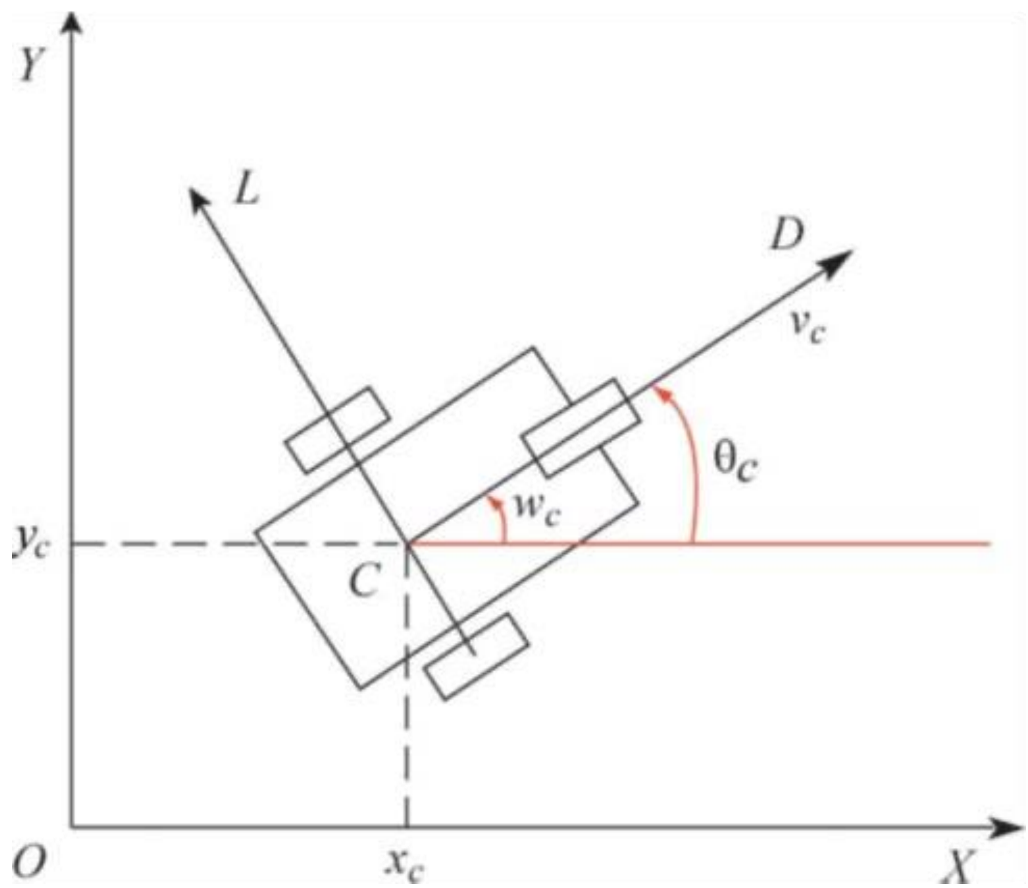

Figure 1: Model of a Non-holonomic mobile robot

The block diagram in Figure 2 depicts the position tracking method for the mobile robot using the bioinspired backstepping controller and the torque controller. A Kalman filter is used to control the linear velocity of the mobile robot. The unscented Kalman filter uses this information to control the position of the mobile robot. Using this idea, we track the robot's path to the desired path.

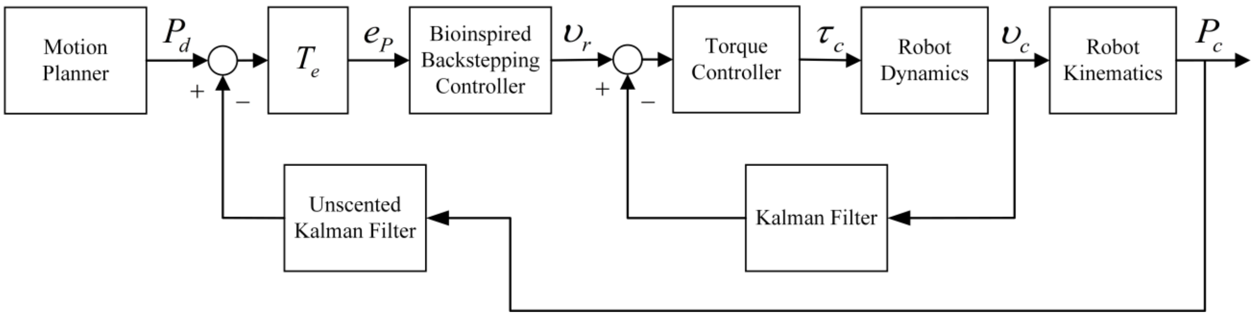

Figure 2: The block diagram of the proposed tracking control with KF and UKF

3. Kinematics of the mobile robot

Let the position of the mobile robot at point C be represented as $\mathrm{P}_c = [\mathrm{x}_c, \mathrm{y}_c, \theta_c]$where x_c & y_c are the spatial position at point C & θ_c is the orientation of the mobile robot at that point. The velocity of the mobile robot can be represented as in Equation (1).

$$\dot{P}_C = \begin{bmatrix} \dot{x}_c \\ \dot{y}_c \\ \dot{z}_c \end{bmatrix}$$

Equation 1: Position determined by forward kinematics

The kinematic constraint to move the robot normal to the driving wheels without slipping is represented as:

$$\dot{y}_c \cos \dot{\theta}_c - \dot{x}_c \sin \dot{\theta}_c = 0$$

Equation 2: Kinematic constraint

These constraints are known as Pfaffian constraints and can be represented as in equation (3).

$$A(P_c)\dot{P}_c = 0$$

Equation 3

The null space of $A(Pc)$ can be represented as in Equation (4).

$$A(Pc) = [-\sin\theta \quad \cos\theta \quad 0]$$

Equation 4

Substituting Equations 1 and 4 in Equation (3) we get Equation (5).

$$[-\sin\theta \quad \cos\theta \quad 0] \begin{bmatrix} \dot{x}_c \\ \dot{y}_c \\ \dot{\theta}_c \end{bmatrix} = 0$$

Equation 5

This would result in two linearly independent vectors which are a basis of the null space of $A(Pc)$ as in equation 6

$$\begin{bmatrix} \dot{x}_c \\ \dot{y}_c \\ \dot{z}_c \end{bmatrix} = \begin{bmatrix} \cos\theta \\ \sin\theta \\ 0 \end{bmatrix} v_c + \begin{bmatrix} 0 \\ 0 \\ 1 \end{bmatrix} \omega_c$$

Equation 6

Thus, the relationship between the velocity of the mobile robot in the initial frame and velocity of the mobile robot in the body fixed frame can be represented as in equation 7 where v_c and ω_c represent the linear and angular velocities.

$$\dot{P}_c = \begin{bmatrix} \dot{x}_c \\ \dot{y}_c \\ \dot{z}_c \end{bmatrix} = \begin{bmatrix} \cos\theta & 0 \\ \sin\theta & 0 \\ 0 & 1 \end{bmatrix} \begin{bmatrix} v_c \\ \omega_c \end{bmatrix}$$

Equation 7: Kinematics of the Mobile Robot

3.1. Dynamics of the mobile robot

Equation of motion for the non-holonomic mobile robot without considering gravity is given as:

$$\overline{M}\,(P_c)\dot{V} + \bar{F}\left(P_c, \dot{P}_c\right) + \overline{\tau_d} = \bar{B}\,\tau_c$$

Equation 8: Equations of motion

The total Kinetic energy is given by equation (9)

$$\mathrm{K.E.} = \frac{1}{2}\,mv^2 + \frac{1}{2}\,I\theta^2$$

Equation 9: Kinetic energy

The Euler Lagrange Equation of motion is given by Equation (10).

$$\frac{d}{dt}\frac{\partial \mathcal{L}}{\partial \dot{q}_j} - \frac{\partial \mathcal{L}}{\partial q_j} = \tau_j$$

Equation 10: Euler Lagrange Equation of motion

Using equation (10) and considering L to be the total Kinetic Energy, the equations of motion can be written as are given as:

$$m\ddot{v} = \tau_r$$

Equation 11

$$I\ddot{\theta} = \tau_L$$

Equation 12

The Positive definite matrix of Inertia and the Centrepetal and Coriolis Matrix are given as in equation (13) where m is the mass of the mobile robot and I is the inertia of the mobile robot.

$$\bar{M} = \begin{bmatrix} m & 0 \\ 0 & I \end{bmatrix}, \bar{F} = \begin{bmatrix} 0 & 0 \\ 0 & 0 \end{bmatrix}$$

Equation 13

The equation of motions can be transformed into a form represented by linear and angular velocities as in equation (14).

$$v_c = {}^1\!/_r\,(\tau_r + \tau_l), \omega_c = {}^l\!/_r\,(\tau_r + \tau_l)$$

Equation 14

From this we can obtain:

$$\bar{B} = \frac{1}{r} \begin{bmatrix} 1 & 1 \\ l & l \end{bmatrix}, \tau_C = \begin{bmatrix} \tau_R \\ \tau_L \end{bmatrix}$$

Equation 10

Here r is the radius of the driving wheels and l is the azimuth length from point C to the driving wheels. τ_R and τ_L are the right and left wheel torque inputs which are obtained from the Torque controller. The mobile robot parameters are set as m = 10, I = 0.1, l = 1, and r = 1.

The simplified dynamics of the mobile robot is expressed as:

$$\dot{V} = \bar{M}^{-1}\,\bar{B}\,.\tau_c$$

Equation 11: Dynamics of the mobile robot

Where $V = [v_c, \omega_c]^T$, v_c and ω_c represent the linear and angular velocities respectively. Integrating $\dot{V}$ in equation (16), will give us V which is used for calculating the Robot Kinematics.

3.2. Kalman Filter (KF)

A linear system with noises is given by the following equations.

$$x_{k+1} = Ax_k + Bu_k + \propto_k$$

Equation 12

$$z_{k+1} = Hx_{k+1} + \beta_{k+1}$$

Equation 13

were A is the system matrix and B is the input matrix, u_k is the input and H is the measurement matrix.

The covariance of the noise models $\propto$ and β is given by the following equations.

$$Q = E[\propto_k, \propto_k^T]$$

Equation 14

$$R = E[\beta_k, \beta_k^T]$$

Equation 15

P_k is error covariance matrix. $P_{k+1/k+1}$ is the posterior state error covariance matrix. $P_{k+1/k}$ is the priori state error covariance matrix. $x_{k+1/k+1}$ is the posterior state estimate and $x_{k+1/k}$ is the priori state estimate.

The expansion of the $P_{k+1/k+1}$ os given by equation (21).

$$P_{k+1/k+1} = E[(x_{k+1/k+1} - x_{k+1/k})(x_{k+1/k+1} - x_{k+1/k})^T]$$

Equation 16

The posterior state estimate is thus given by equation (22) where K_{k+1} is the Kalman gain and the measurement residual is given by equation (23).

$$x_{k+1/K+1} = x_{k+1/k} + K_{k+1}(z_{k+1} - x_{k+1/k})$$

Equation 17

$$i_{k+1} = z_{k+1/k+1} + Hx_{k+1/k}$$

Equation 18

Substituting equation (18) into equation (22) gives equation (24).

$$x_{k+1/k+1} = x_{k+1/k} + K_{k+1}\left(Hx_{k+1/k+1} + \beta_{k+1} - H\mathrm{x}_{k+1/k}\right)$$

Equation 19

Substituting (23), (24) in (21) gives:

$$P_{k+1/k+1} = E\left[\left[(I - K_{k+1}H)\left(x_{k+1/k+1} - \mathrm{x}_{k+1/k}\right) - K_{k+1}\beta_{k+1}\right]\right.$$
$$\left.\left[(I - K_kH)\left(x_{k+1/k+1} - \mathrm{x}_{k+1/k}\right) - K_{k+1}\beta_{k+1}\right]^T\right]$$

Equation 20

Expansion of (25) gives:

$$P_{k+1} = (I - K_{k+1}H)E\left[\left(x_{k+1/k+1} - \mathrm{x}_{k+1/k}\right)\left(x_{k+1/k+1} - \mathrm{x}_{k+1/k}\right)^T\right](I - K_{k+1}H)$$
$$+K_{k+1}E[\beta_{k+1}\beta_{k+1}^T]K_{k+1}^T$$

Equation 21

Substituting (20) and (21) in (25) gives:

$$P_{k+1/k+1} = (I - K_{k+1}H)P_{k+1/k+1}(I - K_{k+1}H)^T + K_{k+1}RK_{k+1}^T$$

Equation 22

Expanding (27) we get:

$$P_{k+1/k+1} = P_{k+1/k} - K_{k+1}HP_{k+1/k} - P_{k+1/k}H^TK_{k+1}^T + K_{k+1}\left(HP_{k+1/k}H^T + R\right)K_{k+1}^T$$

Equation 23

Differentiating the trace of $P_{k+1/k+1}$ with respect to the Klaman gain we can obtain the Kalman gain as in (32).

$$T[P_{k+1/k+1}] = T[P_{k+1/k}] - 2T[K_{k+1}HP_{k+1/k}] + T[K_{k+1}(HP_{k+1/k}H^T + R)K_{k+1}^T]$$

Equation 24

$$\frac{dT[P_{k+1/k+1}]}{dK_{k+1}} = -2(HP_{k+1/k})^T + 2K_{k+1}(HP_{k+1/k}H^T + R)$$

Equation 25

$$(HP_{k+1/k+1})^T = K_{k+1}(HP_{k+1/k}H^T + R)$$

Equation 26

$$K_{k+1} = P_{k+1/k}H^T(HP_{k+1/k}H^T + R_{k+1})^{-1}$$

Equation 27: Kalman Gain

Substituting (32) in (26) gives the updates state error covariance matrix.

$$P_{k+1/k+1} = P_{k+1/k} - P_{k+1/k}H^T(HP_{k+1/k}H^T + R)^{-1}HP_{k+1/k}$$
$$P_{k+1/k+1} = P_{k+1/k} - K_{k+1}HP_{k+1/k}$$
$$P_{k+1/k+1} = (I - K_{k+1}H)P_{k+1/k}$$

Equation 28

3.3. Unscented Kalman Filter (UKF)

The UKF is used to deal with nonlinear systems of the form as in (34)

$$\mathrm{x}_{k+1} = \mathrm{f}(\mathrm{x}_{k,}\mathrm{u}_{k,}) + \delta_k$$
$$\mathrm{z}_{k+1} = \mathrm{h}(\mathrm{x}_{k+1}) + \gamma_{k+1}$$

Equation 29

Sampling points for UKF needs to be generated 2n+1 sampling points called sigma points and n with n being the dimension of x_k. The initial sigma point, and its weight are given by (35) where λ is a design value controlling the spread of sigma points.

$$x_{0,k|k} = \hat{x}_{k|k}$$
$$W_0 = \frac{\lambda}{n+\lambda}$$

Equation 30

The general expression of the sigma point $X_{i,k/k}$ and W_i, and its weight are given by (36)

$$X_{i,k|k} = \hat{x}_{k|k} + \left(\sqrt{(n+\lambda)P_{k|k}}\right)_i$$
$$W_i = \frac{1}{[2(n+\lambda)]}$$

Equation 31

Using equations (34)-(36), the final n sigma points are given as in (37) and the as the state estimate of $x_{k+1/k}$ is given by (38).

$$X_{i+n,k|k} = \hat{x}_{k|k} - \left(\sqrt{(n+\lambda)P_{k|k}}\right)_i$$
$$W_{i+n} = \frac{1}{[2(n+\lambda)]}$$

Equation 32

$$\hat{X}_{i,k+1|k} = f\big(\hat{X}_{i,k|k}, u_k\big)$$
$$\hat{x}_{i,k+1|k} = \sum_{i=0}^{2n} W_i \hat{X}_{i,k+1|k}$$

Equation 33

The predicted state error covariance $P_{k+1|k}$ is given by (39)

$$P_{k+1|k} = \sum_{i=0}^{2n} W_i\big(\hat{X}_{i,k+1|k} - \hat{x}_{k+1|k}\big)\big(\hat{X}_{i,k+1|k}$$
$$-\hat{x}_{k+1|k}\big)^{\mathrm{T}} + Q_k$$

Equation 34

The predicted measurement model is given by (40) where $\hat{Z}_{i,k+1|k}$ and $\hat{z}_{k+1|k}$.

$$\hat{Z}_{i,k+1|k} = h\big(\hat{X}_{i,k+1}, u_k\big)$$
$$\hat{z}_{k+1|k} = \sum_{i=0}^{2n} W_i \hat{Z}_{i,k+1|k}$$

Equation 35

Using (40) the measurement covariance $P_{zz,k+1|k}$ and $P_{xz,k+1|k}$ is given by (41)

$$P_{zz,k+1|k} = \sum_{i=0}^{2n} W_i\big(\hat{Z}_{i,k+1|k} - \hat{z}_{k+1|k}\big)\big(\hat{Z}_{i,k+1|k}$$
$$P_{xz,k+1|k} = \sum_{i=0}^{2n} W_i\big(\hat{X}_{i,k+1|k} - \hat{x}_{k+1|k}\big)\big(\hat{Z}_{i,k+1|k}\big)^{\mathrm{T}} + R_k$$
$$-\hat{z}_{k+1|k}\big)^{\mathrm{T}}$$

Equation 36

Thus, Kalman gain, state estimate and state error covariance is given by (42). The UKF provides accurate estimates for the nonlinear system with noises.

$$K_{k+1} = P_{xz,k+1|k} P_{zz,k+1|k}^{-1}$$
$$\hat{x}_{k+1|k+1} = \hat{x}_{k+1|k} + K_{k+1}(z_{k+1} - \hat{z}_{k+1|k})$$
$$P_{k+1|k+1} = P_{k+1|k} - K_{k+1} P_{zz,k+1|k} K_{k+1}^{\mathrm{T}}$$

Equation 37

3.4. KF and UKF of model robot

Based on equation (8) and (16), knowing the time-step Δt, using the Euler approximation, the KF state for the mobile robot can be defined as

$$\hat{V}_{k+1}^{-} = \begin{bmatrix} \hat{v}_{c,k+1}^{-} \\ \widehat{\omega}_{c,k+1}^{-} \end{bmatrix} = \begin{bmatrix} \hat{v}_{c,k} \\ \widehat{\omega}_{c,k} \end{bmatrix} + \bar{M}^{-1}\bar{B}\tau_{c,k} \cdot \Delta t + \alpha_k$$

Equation 38

Here $\hat{v}_{c,k}$ and $\widehat{\omega}_{c,k}$ are respectively the estimated linear and angular velocity at time k. $\hat{v}_{c,k+1}^{-}$ and $\widehat{\omega}_{c,k+1}^{-}$ are the priori estimates of linear and angular velocities at the time $k+1$, α_k is the system noise of the mobile robot.

The measurement for the dynamics of the mobile robot is calculated as:

$$\tilde{V}_{k+1} = H\left(\hat{V}_{k+1}^{-}, \beta_{k+1}\right) = H \begin{bmatrix} \hat{v}_{c,k+1}^{-} \\ \widehat{\omega}_{c,k+1}^{-} \end{bmatrix} + \beta_{k+1}$$

Equation 39

Here $\tilde{V}_{k+1}$ and β_{k+1} are the measured velocity vector and the measurement noise at time $k+1$, respectively. The mobile robot has system noises due to the sophisticated design.

As for the UKF, the state and measurement model for the kinematics of the mobile robot is treated as:

$$\hat{P}_{c,k+1}^{-} = \begin{bmatrix} \hat{x}_{c,k+1}^{-} \\ \hat{y}_{c,k+1}^{-} \\ \hat{\theta}_{c,k+1}^{-} \end{bmatrix} = \begin{bmatrix} \hat{x}_{c,k} + \cos\hat{\theta}_{c,k}\hat{v}_{c,k}\Delta t \\ \hat{y}_{c,k} + \sin\hat{\theta}_{c,k}\hat{v}_{c,k}\Delta t \\ \hat{\theta}_{c,k} + \widehat{\omega}_{c,k}\Delta t \end{bmatrix} + \delta_k$$

Equation 40

$$\tilde{P}_{c,k+1} = h\left(\hat{P}_{c,k+1}^{-}, \gamma_{k+1}\right) = h \begin{bmatrix} \hat{x}_{c,k+1}^{-} \\ \hat{y}_{c,k+1} \\ \hat{\theta}_{c,k+1}^{-} \end{bmatrix} + \gamma_{k+1}$$

Equation 41

Here $\hat{x}_{c,k}$, $\hat{y}_{c,k}$ and $\hat{\theta}_{c,k}$ are the estimates of the robot positions at time k, $\hat{x}_{c,k+1}^{-}$, $\hat{y}_{c,k+1}$ and $\hat{\theta}_{c,k+1}^{-}$ are the priori estimates of the robot position at time $k+1$.

3.5. Bioinspired Backstepping controller

Equation (47) gives the conventional backstepping tracking control law for nonholonomic mobile robots.

$$v_r = C_1 e_D + v_d \cos e_\theta$$

Equation 42: Conventional backstepping tracking control law

$$\omega_r = \omega_d + C_2 v_d e_L + C_3 v_d \sin e_\theta$$

Equation 43

Here C_1, C_2 and C_3 are the designed parameters. v_r and ω_r are respectively the reference linear and angular velocity command that generated from the controller. Since the control law has a jumping issue, we use a bio inspired backstepping control which uses the dynamics of voltage across the membrane, which is called the shunting model.

$$C_m \frac{dV_m}{dt} = -(E_p + V_m)g_p + (E_{Na} - V_m)g_{Na} - (E_k + V_m)g_K$$

Equation 44

Here C_m is the membrane capacitance, parameters E_p, E_{Na} and E_k are the Nernst potentials for the passive leak, sodium ions and potassium ions in the membrane respectively. The paraments g_p, g_{Na} and g_K denote the conductance of passive channel, sodium, and potassium. This model is the foundation for the shunting model discussed above.

With the implementation of shunting model into conventional backstepping control, the bioinspired backstepping control laws are defined as:

$$v_r = v_s + v_d \cos e_\theta$$
$$\omega_r = \omega_d + C_2 v_d e_L + C_3 v_d \sin e_\theta$$

Equation 45: Bioinspired backstepping controller

Here v_s is from a neural dynamics equation with respect to the error in the driving direction as:

$$\frac{dv_s}{dt} = -A_1 v_s + (B_1 - v_s) f(e_D) - (D_1 + v_s) g(e_D)$$

Equation 46

here $f(e_D) = max\{e_D, 0\}$ is the linear above threshold function and $f(e_D) = max\{-e_D, 0\}$ is a nonlinear function. The parameter A_1 is the passive decay rate and B_1 and D_1 are the upper and lower bound of the velocity, respectively.

The Lyapunov candidate function and its time derivative for bioinspired backstepping control is proposed as:

$$V_1 = \frac{1}{2} e_D^2 + \frac{1}{2} e_L^2 + \frac{1}{C_2}(1 - \cos e_\theta) + \frac{1}{2B_1} v_s^2$$
$$\dot{V}_1 = \dot{e}_D e_D + \dot{e}_L e_L + \frac{1}{C_2} \dot{e}_\theta \sin e_\theta + \frac{1}{B_1} \dot{v}_s v_s$$

Equation 47

3.6. Torque Controller

The actual velocity of the mobile robot is different from the velocity command generated from the bioinspired backstepping control due to noises. The velocity tracking error e_η is expressed as:

$$e_\eta = \begin{bmatrix} e_v \\ e_\omega \end{bmatrix} = \begin{bmatrix} v_r - v_c \\ \omega_r - \omega_c \end{bmatrix}$$

Equation 48

Then the torque tracking control low $\tau_L = [\tau_L, \ \tau_R]^T$ is proposed as:

$$\tau_L = \frac{mr}{2}(\dot{v}_r + C_4 e_v) - \frac{Ir}{2c}(\dot{\omega}_r + C_5 e_\omega)$$
$$\tau_R = \frac{mr}{2}(\dot{v}_r + C_4 e_v) + \frac{Ir}{2c}(\dot{\omega}_r + C_5 e_\omega)$$
Equation 49

The Lyapunov candidate function and its time derivate for torque controller can be defined as:

$$V_2 = V_1 + \frac{1}{2}{e_v}^2 + \frac{1}{2}{e_\omega}^2$$
$$\dot{V}_2 = \dot{V}_1 + e_v \dot{e}_v + e_\omega \dot{e}_\omega = \dot{V}_1 + e_v(\dot{v}_r - \dot{v}_c) + e_\omega(\dot{\omega}_r - \dot{\omega}_c)$$
Equation 50

3.7. Stability Analysis

To prove the stability of the proposed control strategy, the bioinspired backstepping controller and torque controller are firstly proven to be asymptotically stable. The overall stability is then proven as well. From equation (52), $\dot{V}_1$ can be rewritten as:

$$\dot{V}_1 = -v_s e_D - \frac{C_3}{C_2} v_d \sin^2 \, e_\theta + \frac{1}{B_1}[-A_1 - f(e_D) - g(e_D)]v_s^2 + \frac{1}{B_1}[B_1 f(e_D) - D_1 g(e_D)]v_s$$
Equation 51

Assuming $B_1 = D_1$, equation (56) can be rewritten as:

$$\dot{V}_1 = -\frac{C_3}{C_2} v_d \sin^2 e_\theta + \frac{1}{B_1}[-A_1 - f(e_D) - g(e_D)]v_s^2 + [f(e_D) - g(e_D) - e_D]v_s$$
Equation 52

From the definition of $f(e_D)$ and $g(e_D)$. If $e_D \geq 0$, $f(e_D) = e_D$ and $g(e_D) = 0$, similarly when $e_D \leq 0$, $f(e_D) = 0$ and $g(e_D) = e_D$. Using these conditions, we get:

$$[f(e_D) - g(e_D) - e_D]v_s = e_D - 0 - e_D = 0$$
$$[f(e_D) - g(e_D) - e_D]v_s = 0 - (-e_D) - e_D = 0$$
Equation 53

Using this equation (57) become:

$$\dot{V}_1 = -\frac{C_3}{C_2} v_d \sin^2 e_\theta + \frac{1}{B_1}[-A_1 - f(e_D) - g(e_D)]v_s^2$$
Equation 54

The C_3, C_2 and v_d are positive constants, $g(e_D)$ and $f(e_D)$ are nonnegative, and A_1 and B_1 are nonnegative constants. Therefore $\dot{V}_1 \leq 0$, if and only if $e_D = 0$ and $e_\theta = 0$, then $\dot{V}_1 = 0$, thus torque controller is asymptotically stable.

To prove the stability of the torque controller, use equation (16) in equation (55)

$$\dot{V}_2 = \dot{V}_1 + e_v\left(\dot{v}_r - \frac{1}{mr}\tau_L - \frac{1}{mr}\tau_R\right) + e_\omega\left(\dot{\omega}_r + \frac{l}{Ir}\tau_L - \frac{l}{Ir}\tau_R\right)$$

Equation 55

By replacing τ_L and τ_R from equation (54) in equation (60), $\dot{V}_2$ changes to

$$\dot{V}_2 = \dot{V}_1 - C_4{e_v}^2 - C_5{e_\omega}^2$$

Equation 56

Since $\dot{V}_1$, $-C_4{e_v}^2$ and $-C_5{e_\omega}^2$ are either less than or equal to zero, the torque controller reaches a stable condition, If and only if e_D, e_θ and e_η are zero. If e_D, e_θ and e_η are zeros, then $\dot{V}_2 = 0$, which means that the torque control is asymptotically stable. For the overall stability analysis, the Lyapunov candidate function of the system can be defined as:

$$V_3 = V_1 + V_2$$

Equation 57

The time derivative of V_3 is given by:

$$\dot{V}_3 = 2\left(-\frac{C_3}{C_2}v_d\sin^2 e_\theta + \frac{1}{B_1}[-A_1 - f(e_D) - g(e_D)]\right) - C_4{e_v}^2 - C_5{e_\omega}^2$$

Equation 58

The above condition is true when e_P and e_η are zeros which means $\dot{V}_3 = 0$. Therefore when $e_\theta = [-\pi,\ \pi]$, the entire system is globally asymptotically stable.

4. Implementation & Simulations

4.1. SIMULINK modelling

The equations from literature review are modelled using SIMULINK. Figure 3 consists of the designed model equivalent to the block diagram in the earlier section. The inputs and outputs of each block have been computed as per the equations in the different sections.

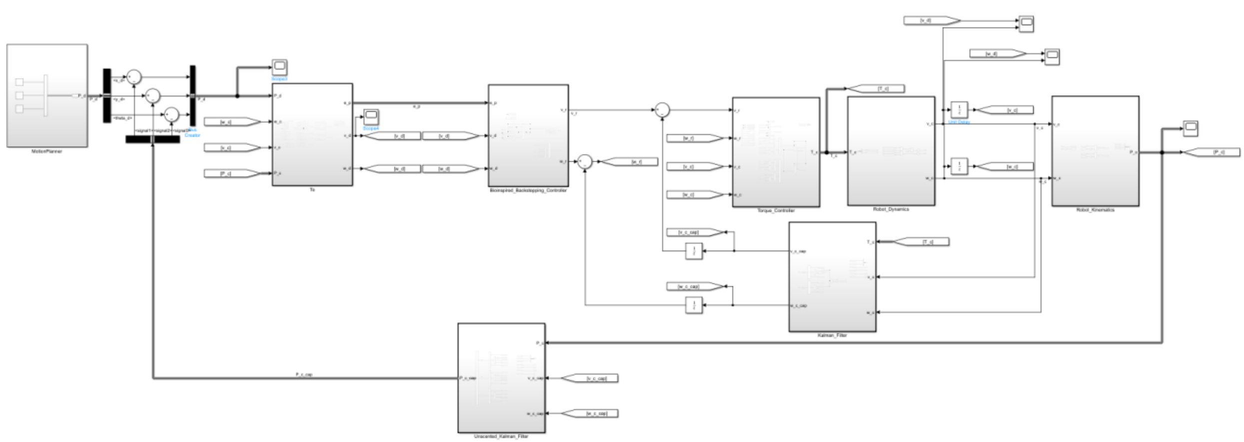

Figure 3: SIMULINK model for Bioinspired backstepping mobile robot

For example, the input to the backstepping controller as in Figure 4 is the error dynamics given by $e^{\cdot}_p$ along with v$_d$ and ω_d. e_p is calculated through a transformation matrix as in (64).

$$e_P = \begin{bmatrix} e_D \\ e_L \\ e_\theta \end{bmatrix} = \begin{bmatrix} \cos\ \theta_c & \sin\ \theta_c & 0 \\ -\sin\ \theta_c & \cos\ \theta_c & 0 \\ 0 & 0 & 1 \end{bmatrix} \begin{bmatrix} e_x \\ e_y \\ e_\theta \end{bmatrix}$$

Equation 64

The error dynamics is obtained by taking the derivative of (64) where $e_x = x_d - x_c, e_y = y_d - y_c$, and $e_\theta = \theta_d - \theta_c$.

$$\begin{bmatrix} \dot{e}_D \\ \dot{e}_L \\ \dot{e}_\theta \end{bmatrix} = \begin{bmatrix} \omega_c e_L - v_c + v_d \cos\ e_\theta \\ -\omega_c e_D + v_d \sin\ e_\theta \\ \omega_d - \omega_c \end{bmatrix}$$

Equation 65

The desired linear and angular velocity is given by (66)

$$v_d = \sqrt{x_d^2 + y_d^2}$$

$$\omega_d = \frac{\ddot{y}_d \dot{x}_d - \ddot{x}_d \dot{y}_d}{\dot{x}_d^2 + \dot{y}_d^2}$$

Equation 66

Figure 4 shows e_p, v$_d$ and ω_d as input to the bioinspired backstepping controller and v$_r$ and ω_r are the output response.

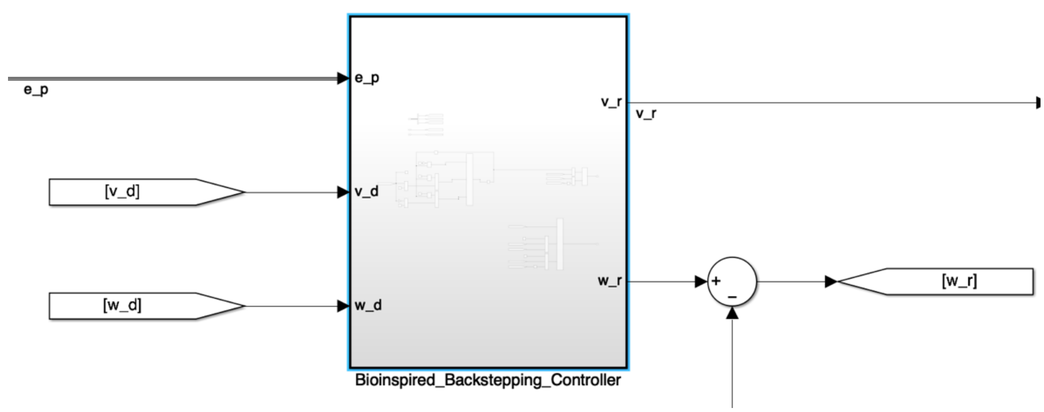

Figure 4: SIMULINK model for Bioinspired backstepping mobile robot

In the case of the Kalman filter, the velocity v_d *and* ω_d obtained from the calculations of the robot dynamics are input to the Kalman filter and the estimated velocity of the backstepping controller is the output response.

Figure 5 depicts the Kalman filter modelled as per (43) with respect to the robot dynamics and torques of the left and right wheels respectively. The output response is the estimated linear and angular velocities of the mobile robot.

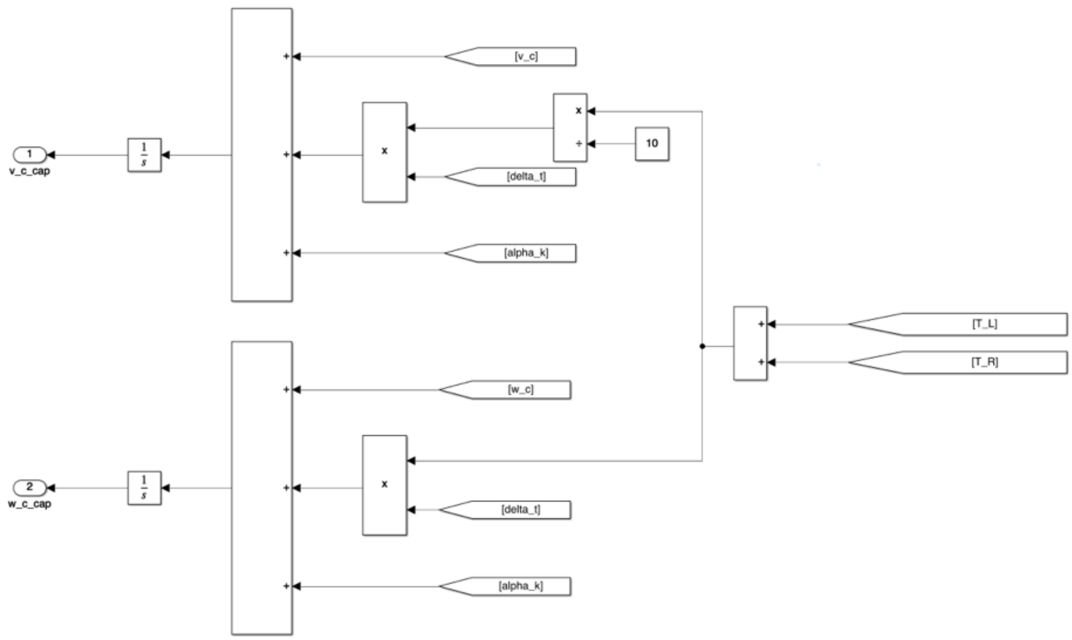

Figure 5: Kalman Filter Design

Figure 6 depicts the design of the UKF which estimates the position of the robot at different time instances based on the measured position as in equation (45).

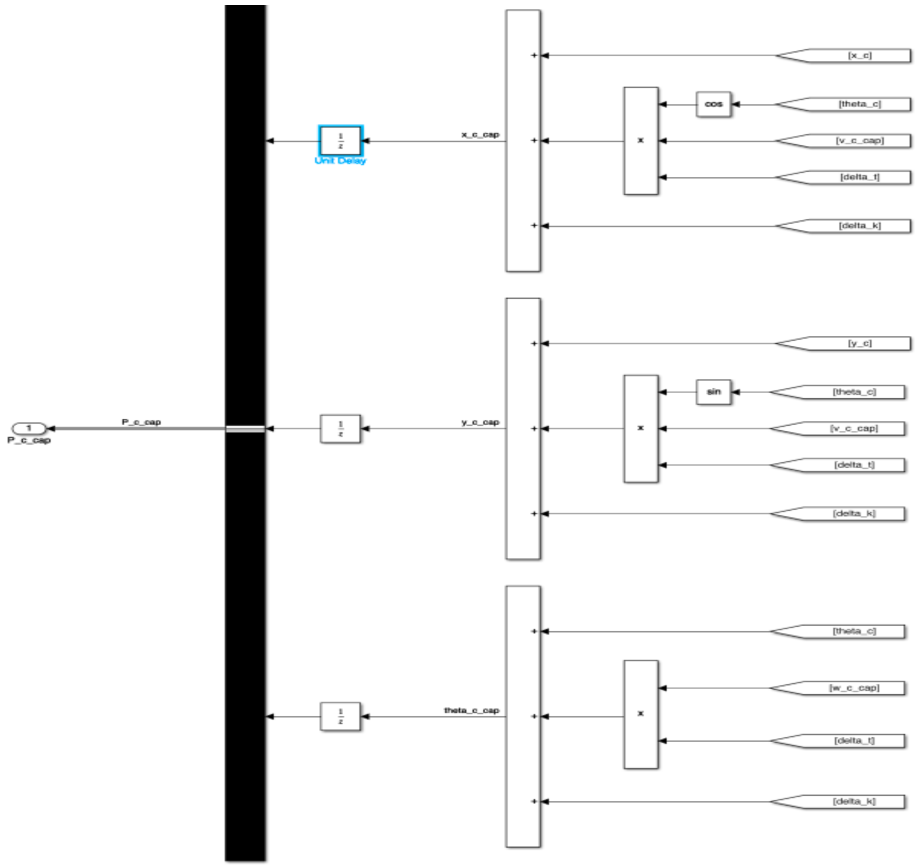

Figure 6: Unscented Kalman Filter Design

4.2. Simulation results

Simulations were performed in the case of a robot travelling in a straight path with an initial position of (0,3) and the desired path as x=0 and y=4. The parameters of the bioinspired backstepping controllers and the torque controllers were given as C2=5, C3=2, A1=5, B1=3, D1=3, C4=5 and C5=5.

Figure 7 shows the plot of the estimated posture of the robot over the time interval of 10 secs. The estimated posture slowly increases from y=0 to y=2.5 and saturates. The desired posture would be obtained when a value of y=4 is obtained. Efforts were taken to tune the controller accordingly, but we were unable to achieve the desired posture at y=4.

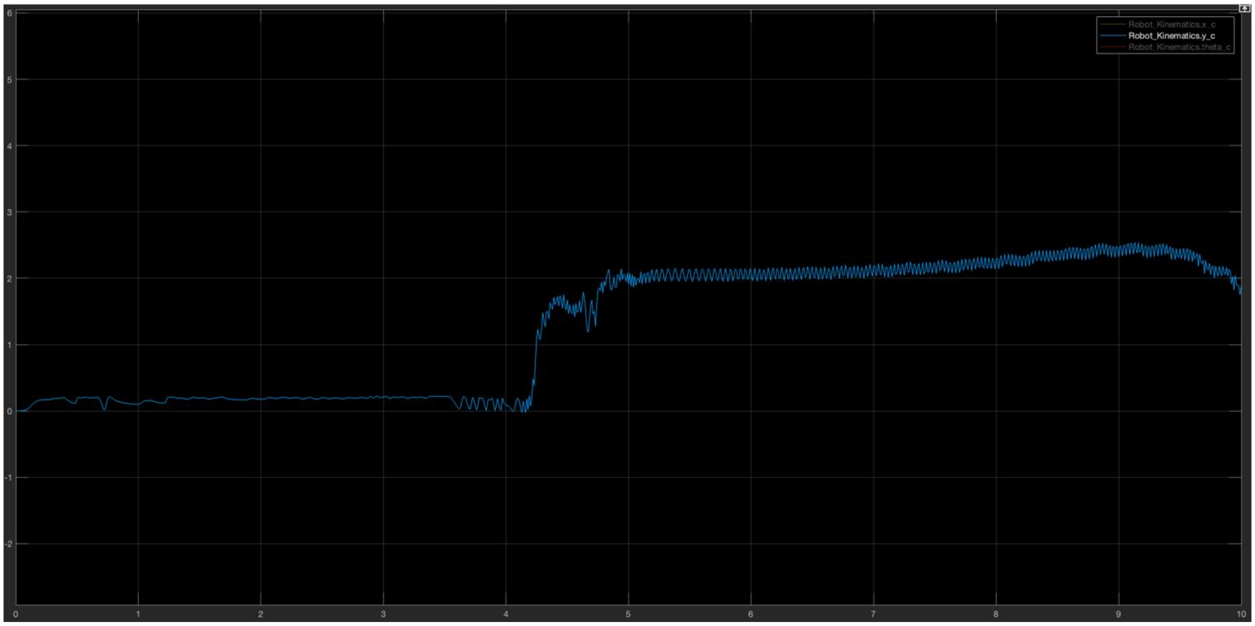

Figure 8 shows the plot of the estimated linear velocity (in blue) and the desired linear velocity (yellow). There is a lot of difference initially but improves overtime.

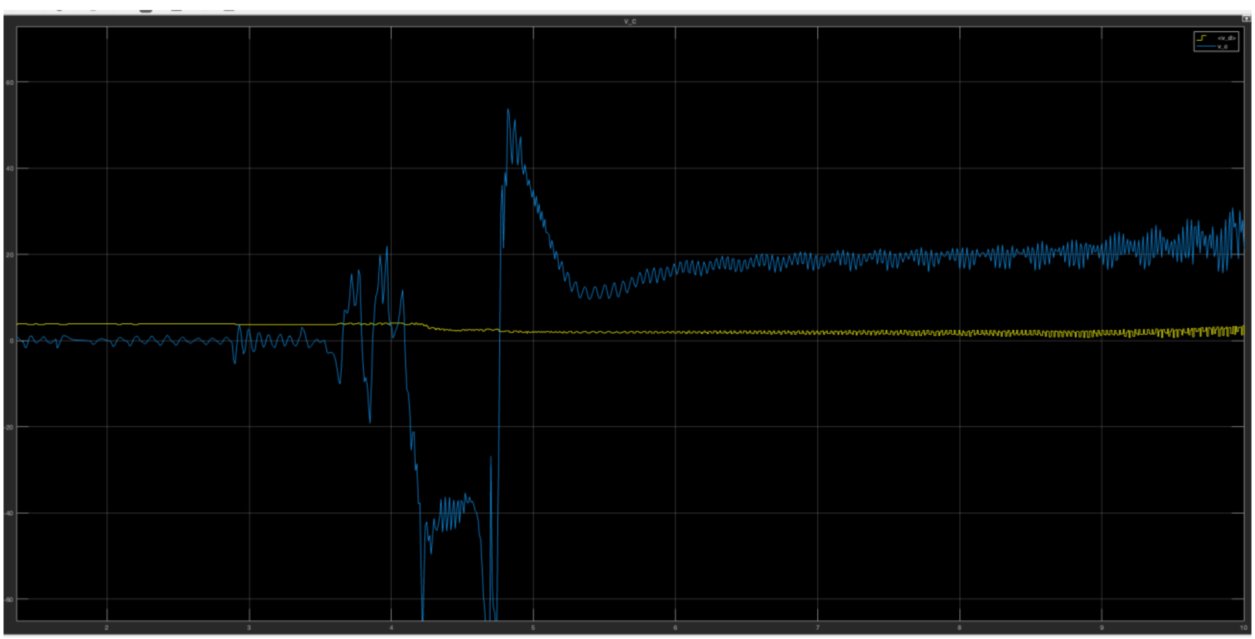

Similarly Figure 9 shows the plot for the estimated angular velocity and the desired angular velocity which behaves the same way as the previous case with a lot of difference initially and the difference between the two values improving overtime.

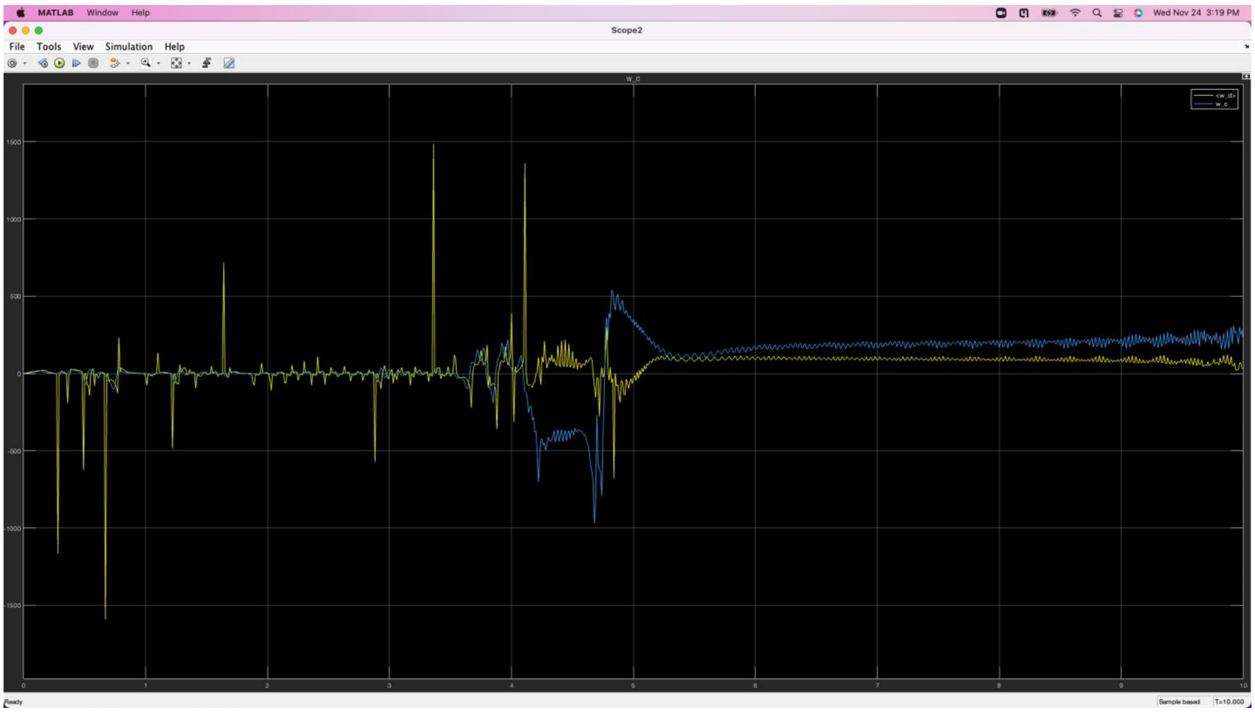

5. Conclusion

The report covers a control strategy to track the direction of the mobile robot when travelling in a straight line using a bioinspired approach. Two controllers have been implemented one is a backstepping controller and the other is a torque controller. The equations describing the various blocks of the model have been derived. The controller model has been designed in Simulink based on the equations of the subsections of the model and simulation has been carried out to track the position of the robot, linear and angular velocity of the mobile robot over a period of time.

References

1. Z. Xu, S. X. Yang and S. A. Gadsden, "Enhanced Bioinspired Backstepping Control for a Mobile Robot With Unscented Kalman Filter," in IEEE Access, vol. 8, pp. 125899-125908, 2020, doi: 10.1109/ACCESS.2020.3007881.
2. https://web.mit.edu/kirtley/kirtley/binlustuff/literature/control/Kalman%20filter.pdf
3. https://stanfordasl.github.io/aa274a/pdfs/notes/lecture1.pdf
4. http://www.cpdee.ufmg.br/~torres/wp-content/uploads/2018/02/nonholonomic_constraints.pdf

5. https://www.hilarispublisher.com/open-access/dynamic-modelling-of-differentialdrive-mobile-robots-using-lagrange-and-newtoneuler-methodologies-a-unified-framework-2168-9695.1000107.pdf
6. https://stats.stackexchange.com/questions/86075/kalman-filter-equation-derivation
7. https://missingueverymoment.wordpress.com/2019/12/02/derivation-of-kalman-filter/
8. https://www.cse.sc.edu/~terejanu/files/tutorialUKF.pdf
9. https://groups.seas.harvard.edu/courses/cs281/papers/unscented.pdf
10. https://math.stackexchange.com/questions/3066305/derivation-of-kalman-gain-for-the-unscented-kalman-filter-ukf